



TESS Data Release Notes:

Sector 21, DR29

Michael M. Fausnaugh, Christopher J. Burke

*Kavli Institute for Astrophysics and Space Science, Massachusetts Institute of Technology,
Cambridge, Massachusetts*

Douglas A. Caldwell

SETI Institute, Mountain View, California

Jon M. Jenkins

NASA Ames Research Center, Moffett Field, California

Jeffrey C. Smith, Joseph D. Twicken

SETI Institute, Mountain View, California

Roland Vanderspek

*Kavli Institute for Astrophysics and Space Science, Massachusetts Institute of Technology,
Cambridge, Massachusetts*

John P. Doty

Noqi Aerospace Ltd, Billerica, Massachusetts

Eric B. Ting

Ames Research Center, Moffett Field, California

Joel S. Villaseñor

*Kavli Institute for Astrophysics and Space Science, Massachusetts Institute of Technology,
Cambridge, Massachusetts*

NASA STI Program ... in Profile

Since its founding, NASA has been dedicated to the advancement of aeronautics and space science. The NASA scientific and technical information (STI) program plays a key part in helping NASA maintain this important role.

The NASA STI program operates under the auspices of the Agency Chief Information Officer. It collects, organizes, provides for archiving, and disseminates NASA's STI. The NASA STI program provides access to the NTRS Registered and its public interface, the NASA Technical Reports Server, thus providing one of the largest collections of aeronautical and space science STI in the world. Results are published in both non-NASA channels and by NASA in the NASA STI Report Series, which includes the following report types:

- **TECHNICAL PUBLICATION.** Reports of completed research or a major significant phase of research that present the results of NASA Programs and include extensive data or theoretical analysis. Includes compilations of significant scientific and technical data and information deemed to be of continuing reference value. NASA counterpart of peer-reviewed formal professional papers but has less stringent limitations on manuscript length and extent of graphic presentations.
- **TECHNICAL MEMORANDUM.** Scientific and technical findings that are preliminary or of specialized interest, e.g., quick release reports, working papers, and bibliographies that contain minimal annotation. Does not contain extensive analysis.
- **CONTRACTOR REPORT.** Scientific and technical findings by NASA-sponsored contractors and grantees.

- **CONFERENCE PUBLICATION.** Collected papers from scientific and technical conferences, symposia, seminars, or other meetings sponsored or co-sponsored by NASA.
- **SPECIAL PUBLICATION.** Scientific, technical, or historical information from NASA programs, projects, and missions, often concerned with subjects having substantial public interest.
- **TECHNICAL TRANSLATION.** English-language translations of foreign scientific and technical material pertinent to NASA's mission.

Specialized services also include organizing and publishing research results, distributing specialized research announcements and feeds, providing information desk and personal search support, and enabling data exchange services.

For more information about the NASA STI program, see the following:

- Access the NASA STI program home page at <http://www.sti.nasa.gov>
- E-mail your question to help@sti.nasa.gov
- Phone the NASA STI Information Desk at 757-864-9658
- Write to:
NASA STI Information Desk
Mail Stop 148
NASA Langley Research Center
Hampton, VA 23681-2199



TESS Data Release Notes:

Sector 21, DR29

Michael M. Fausnaugh, Christopher J. Burke

*Kavli Institute for Astrophysics and Space Science, Massachusetts Institute of Technology,
Cambridge, Massachusetts*

Douglas A. Caldwell

SETI Institute, Mountain View, California

Jon M. Jenkins

NASA Ames Research Center, Moffett Field, California

Jeffrey C. Smith, Joseph D. Twicken

SETI Institute, Mountain View, California

Roland Vanderspek

*Kavli Institute for Astrophysics and Space Science, Massachusetts Institute of Technology,
Cambridge, Massachusetts*

John P. Doty

Noqi Aerospace Ltd, Billerica, Massachusetts

Eric B. Ting

Ames Research Center, Moffett Field, California

Joel S. Villaseñor

*Kavli Institute for Astrophysics and Space Science, Massachusetts Institute of Technology,
Cambridge, Massachusetts*

Acknowledgements

These Data Release Notes provide information on the processing and export of data from the Transiting Exoplanet Survey Satellite (TESS). The data products included in this data release are full frame images (FFIs), target pixel files, light curve files, collateral pixel files, cotrending basis vectors (CBVs), and Data Validation (DV) reports, time series, and associated xml files.

These data products were generated by the TESS Science Processing Operations Center (SPOC, [Jenkins et al., 2016](#)) at NASA Ames Research Center from data collected by the TESS instrument, which is managed by the TESS Payload Operations Center (POC) at Massachusetts Institute of Technology (MIT). The format and content of these data products are documented in the [Science Data Products Description Document \(SDPDD\)](#)¹. The SPOC science algorithms are based heavily on those of the Kepler Mission science pipeline, and are described in the Kepler Data Processing Handbook ([Jenkins, 2017](#)).² The Data Validation algorithms are documented in [Twicken et al. \(2018\)](#) and [Li et al. \(2019\)](#). The [TESS Instrument Handbook](#) ([Vanderspek et al., 2018](#)) contains more information about the TESS instrument design, detector layout, data properties, and mission operations.

The TESS Mission is funded by NASA's Science Mission Directorate.

This report is available in electronic form at
<https://archive.stsci.edu/tess/>

¹<https://archive.stsci.edu/missions/tess/doc/EXP-TESS-ARC-ICD-TM-0014.pdf>

²<https://archive.stsci.edu/kepler/manuals/KSCI-19081-002-KDPH.pdf>

1 Observations

TESS Sector 21 observations include physical orbits 49 and 50 of the spacecraft around the Earth. Data collection was paused for 0.93 days between the orbits to download data. An instrument reset also occurred in orbit 50—no data were collected for two minutes between TJD 1892.50598 and 1892.50875. In total, there are 24.42 days of science data collected in Sector 21.

Table 1: Sector 21 Observation times

	UTC	TJD ^a	Cadence #
Orbit 49 start	2020-01-21 22:15:22	1870.42885	462941
Orbit 49 end	2020-02-04 11:47:22	1883.99273	472707
Orbit 50 start	2020-02-05 10:01:22	1884.91912	473374
Orbit 50 end	2020-02-18 06:41:21	1897.78023	482634

^a TJD = TESS JD = JD - 2,457,000.0

The spacecraft was pointing at RA (J2000): 171.7951°; Dec (J2000): +65.1924°; Roll: −42.0505°. Two-minute cadence data were collected for 20,000 targets, and full frame images were collected every 30 minutes. See the TESS project [Sector 21 observation page](#)³ for the coordinates of the spacecraft pointing and center field-of-view of each camera, as well as the detailed target list. Fields-of-view for each camera and the Guest Investigator two-minute target list can be found at the TESS Guest Investigator Office [observations status page](#)⁴.

1.1 Notes on Individual Targets

Five bright stars ($T_{\text{mag}} \lesssim 1.8$) with large pixel stamps were not processed in the photometric pipeline. Target pixel files with raw data are provided, but no light curves were produced. The affected TIC IDs are 229540730, 157847644, 329269366, 150226696, and 8172111.

Four target stars (341873045, 471011933, 229686919, and 229686929) are blended with comparably bright stars—the contaminating flux for these objects is very large, and the resulting photometry for such targets is expected to be unreliable.

One target (87974462) had a pixel stamp that did not fully capture the bleed trails.

1.2 Spacecraft Pointing and Momentum dumps

Camera 1 and Camera 4 were both used for guiding in orbit 49; Camera 4 alone was used for guiding in orbit 50. The reaction wheel speeds were reset with momentum dumps every 6.25 days (orbit 49) or 6.5 days (orbit 50). Figure 1 summarizes the pointing performance over the course of the sector based on Fine Pointing telemetry.

³<https://tess.mit.edu/observations/sector-21>

⁴<https://heasarc.gsfc.nasa.gov/docs/tess/status.html>

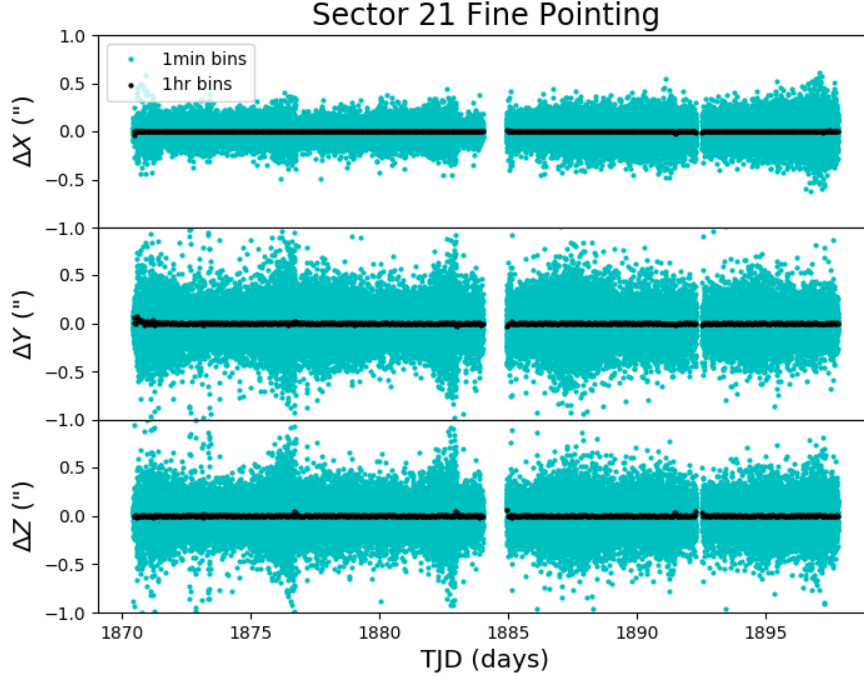


Figure 1: Guiding corrections based on spacecraft fine pointing telemetry. The delta-quaternions from each camera have been converted to spacecraft frame, binned to 1 minute and 1 hour, and averaged across cameras. Long-term trends (such as those caused by differential velocity aberration) have also been removed. The $\Delta X/\Delta Y$ directions represent offsets along the detectors' rows/columns, while the ΔZ direction represents spacecraft roll.

1.3 Scattered Light

Figure 2 shows the median value of the background estimate for all targets on a given CCD as a function of time. Figure 3 shows the angle between each camera's boresight and the Earth or Moon—this figure can be used to identify periods affected by scattered light and the relative contributions of the Earth and Moon to the image backgrounds.

In Sector 21, the Moon passes through the field of view of Camera 1 at the start of orbit 50, saturating the detectors. A strong glint also appears in Camera 2 during this time.

2 Data Anomaly Flags

See the [SDPDD](#) (§9) for a list of data quality flags and the associated binary values used for TESS data, and the [TESS Instrument Handbook](#) for a more detailed description of each flag.

The following flags were not used in Sector 21: bits 1, 2, 7, 9, and 11 (Attitude Tweak, Safe Mode, Cosmic Ray in Aperture, Discontinuity, Cosmic Ray in Collateral Pixel).

Cadences marked with bits 3, 4, 6, and 12 (Coarse Point, Earth Point, Reaction Wheel Desaturation Event, and Straylight) were marked based on spacecraft telemetry.

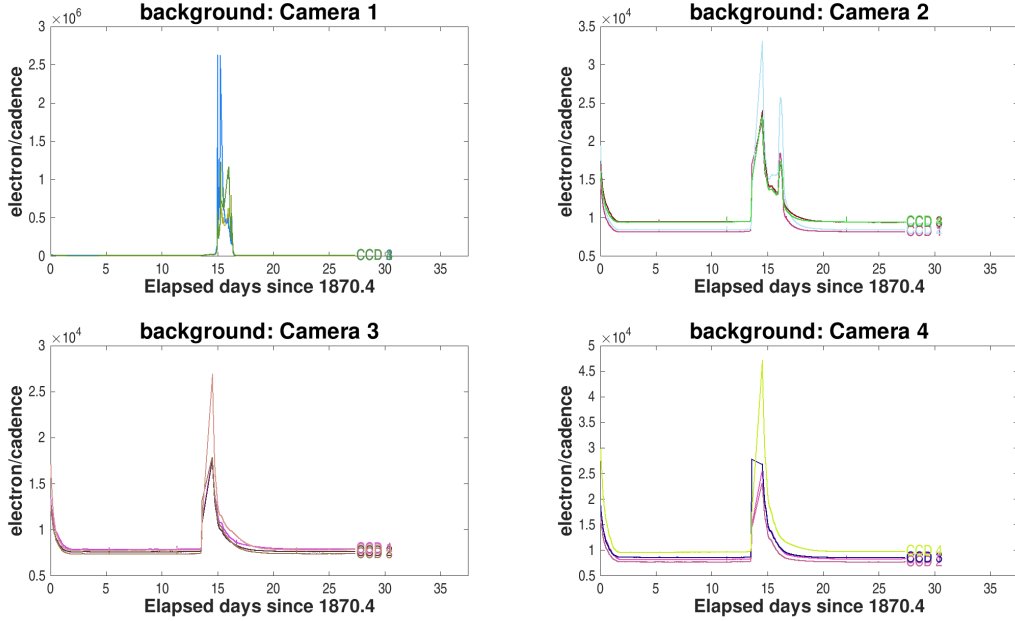


Figure 2: Median background flux across all targets on a given CCD in each camera. The changes are caused by variations in the orientation and distance of the Earth and Moon.

Cadences marked with bit 5 and 10 (Argabrightening Events and Impulsive Outlier) were identified by the SPOC pipeline. Bit 5 marks a sudden change in the background measurements. In practice, bit 5 flags are caused by rapidly changing glints and unstable pointing at times near momentum dumps. Bit 10 marks an outlier identified by PDC and omitted from the cotrending procedure.

Cadences marked with bit 8 (Manual Exclude) are ignored by PDC, TPS, and DV for cotrending and transit searches. In Sector 21, these cadences were identified using spacecraft telemetry from the fine pointing system. All cadences with pointing excursions >7 arcseconds (~ 0.3 pixel) were flagged for manual exclude. See Figure 4 for an assessment of the performance of the cotrending based on the final set of manual excludes.

The Straylight flag (bit 12, value 2048) marks cadences during which stray light from the Earth and Moon are predicted to potentially interfere with spacecraft guidance. We have found that this flag is a very conservative prediction of the impact of stray light on data quality, as stray light affects different parts of the camera FOV at different levels. Instead, starting in Sector 20, we have implemented a “scattered light flag” (bit 13, value 4096) that identifies cadences at which individual targets are affected by scattered light. Cadences are flagged for periods of time where the measured background rises above the baseline background level by a factor of two and where the measured background exceeds a specified fraction of the target flux (0.25 in Sector 21). We strongly recommend that users use bit 13 over bit 12 when removing any cadences from their analyses based on stray light.

If the Earth/Moon interference is strong enough to saturate the detector, all targets on a CCD slice will be affected and the data are unusable. Cadences with bad calibrations due to saturation are now explicitly marked with bit 15 (value 16384, “Bad Calibration Exclude”).

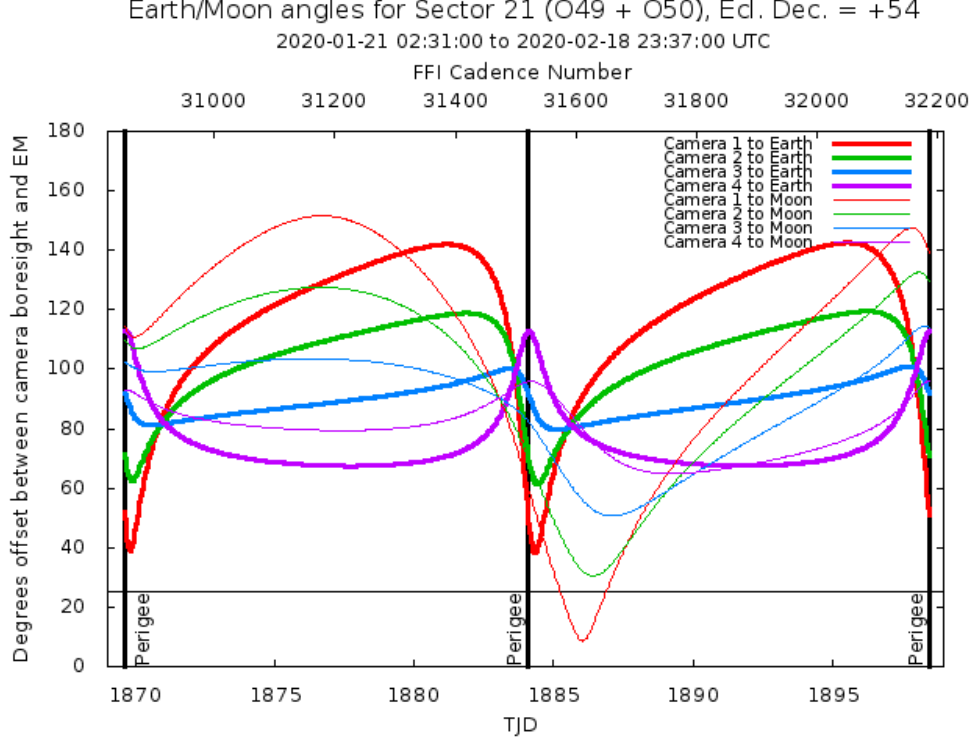


Figure 3: Angle between the four camera boresights and the Earth/Moon as a function of time. When the Earth is within $\sim 25^\circ$ of a camera’s boresight, transiting planet searches may be compromised by high levels of scattered light. At larger angles, up to $\sim 35^\circ$, scattered light patterns and complicated structures may be visible. At yet larger angles, low level patchy features may be visible. Scattered light from the Moon is generally only noticeable below $\sim 35^\circ$. This figure can be used to identify periods affected by scattered light and the relative contributions of the Earth and Moon to the background. However, the background intensity and locations of scattered light features depend on additional factors, such as the Earth/Moon azimuth and distance from the spacecraft.

For some cadences, the majority of targets on a CCD may be flagged for scattered light and not enough valid data remains to derive cotrending basis vectors in PDC. No systematic error correction can be applied at these times. This situation is identified by bit 16 (value 32768, “Insufficient Targets for Error Correction Exclude”).

FFIs were only marked with bits 3, 6 and 12 (Course Point, Reaction Wheel Desaturation Events and Straylight). Only one FFI is affected by each momentum dump. There are no WCS coordinates for FFIs that coincide with momentum dumps.

3 Anomalous Effects

3.1 Smear Correction Issues

The following column was impacted by a bright star in the science frame, and/or upper buffer rows, which bleeds into the upper serial register resulting in an overestimated smear

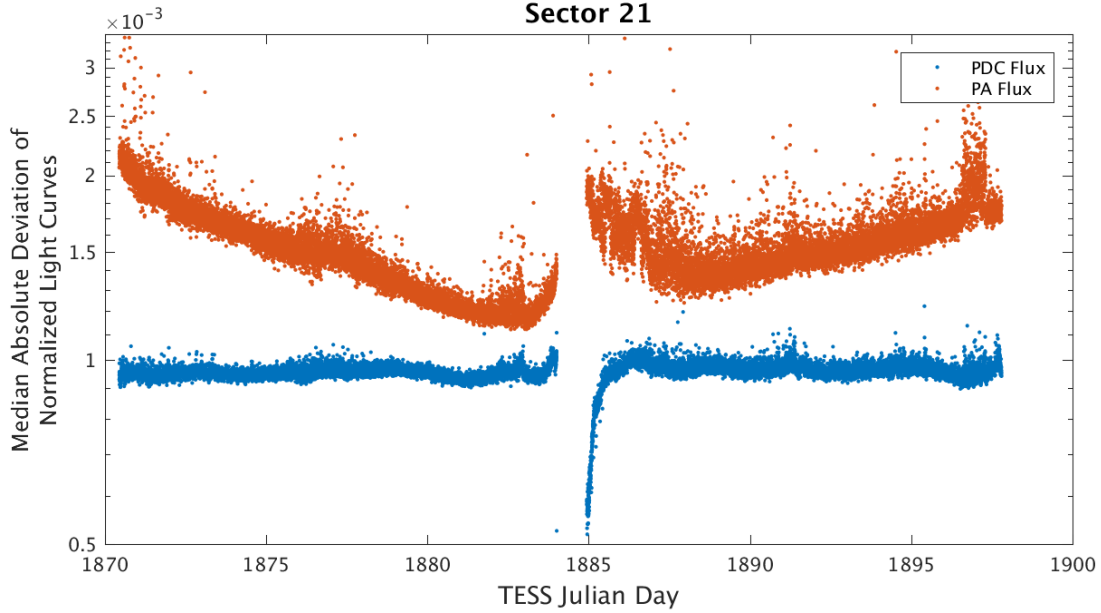


Figure 4: Median absolute deviation (MAD) for the 2-minute cadence data from Sector 21, showing the performance of the cotrending after identifying Manual Exclude data quality flags. The MAD is calculated in each cadence across stars with flux variations less than 1% for both the PA (red) and PDC (blue) light curves, where each light curve is normalized by its median flux value. The scatter in the PA light curves is much higher than that for the PDC light curves, and the outliers in the PA light curves are largely absent from the PDC light curves due to the use of the anomaly flags.

correction.

- Camera 4, CCD 1, Column 1889, Star HD 167469

3.2 Fireflies and Fireworks

Table 2 lists all firefly and fireworks events for Sector 21. These phenomena are small, spatially extended, comet-like features in the images—created by sunlit particles in the camera FOV—that may appear one or two at a time (fireflies) or in large groups (fireworks). See the [TESS Instrument Handbook](#) for a more complete description.

3.3 Corrections to Data Product Timestamps

In Sector 21, the the FFI timestamps have been adjusted for the 0.5 second staggered readouts of the four cameras and the 0.02 second staggered readouts for individual CCDs within a camera. As a reminder, TSTART and TSTOP in the FFIs of previous sectors need to be adjusted for the readout offsets of each camera—see DRN 25 for additional details.

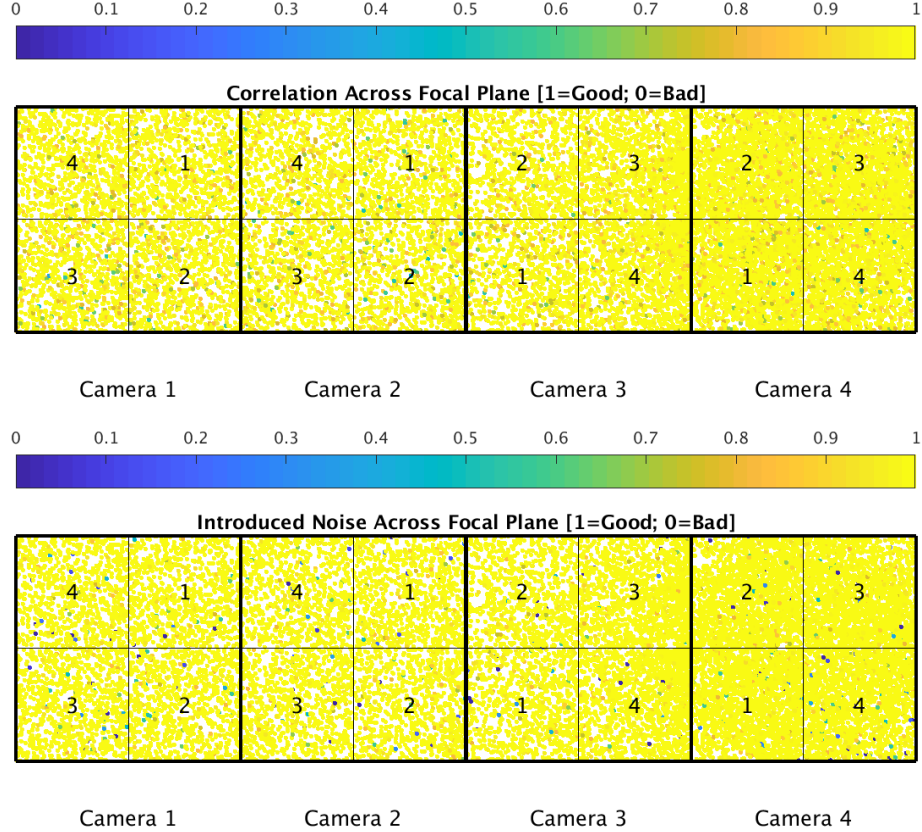


Figure 5: PDC residual correlation goodness metric (top panel) and PDC introduced noise goodness metric (bottom panel). The metric values are shown on a focal plane map indicating the camera and CCD location of each target. The correlation goodness metric is calibrated such that a value greater than 0.8 means there is less than 10% mean absolute correlation between the target under study and all other targets on the CCD. The introduced noise metric is calibrated such that a value greater than 0.8 means the power in broad-band introduced noise is below the level of uncertainties in the flux values.

4 Pipeline Performance and Results

4.1 Light Curves and Photometric Precision

Figure 5 gives the PDC goodness metrics for residual correlation and introduced noise on a scale between 0 (bad) and 1 (good). The performance of PDC is very good and generally uniform over most of the field of view. Figure 6 shows the achieved Combined Differential Photometric Precision (CDPP) at 1-hour timescales for all targets.

4.2 Transit Search and Data Validation

In Sector 21, the light curves of 19995 targets were subjected to the transit search in TPS. Of these, Threshold Crossing Events (TCEs) at the 7.1σ level were generated for 638 targets.

We employed an iterative method when conducting the Sector 21 transit search. The

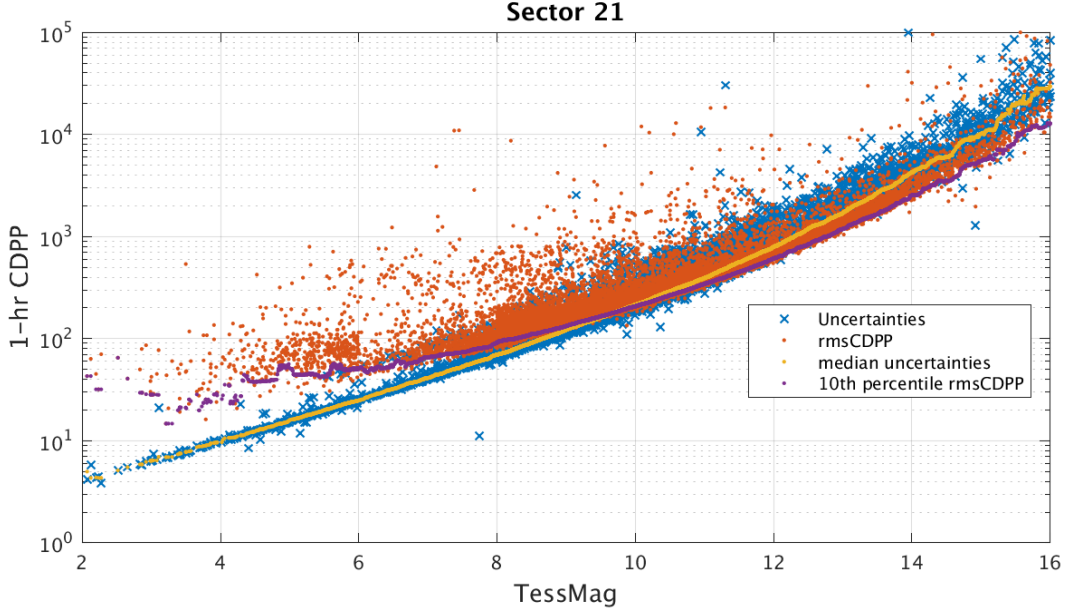


Figure 6: 1-hour CDPP. The red points are the RMS CDPP measurements for the 19995 light curves from Sector 21 plotted as a function of TESS magnitude. The blue x’s are the uncertainties, scaled to 1-hour timescale. The purple curve is a moving 10th percentile of the RMS CDPP measurements, and the gold curve is a moving median of the 1-hr uncertainties.

top panel of Figure 7 shows the number of TCEs at a given cadence that exhibit a transit signal from an initial run of TPS. The 3σ peaks were used to define deemphasis weights for a second run of TPS, the results of which are shown in the bottom panel of Figure 7. The final set of TCEs and the results reported here are based on the second run of TPS. The values of the adopted deemphasis weights are provided in the DV timeseries data products for targets with TCEs.

The top panel of Figure 8 shows the distribution of orbital periods for the final set of TCEs found in Sector 21. The vertical histogram in the right panel of Figure 8 shows the distribution of transit depths derived from limb-darkened transiting planet model fits for TCEs. The model transit depths range down to the order of 100 ppm, but the bulk of the

Table 2: Sector Fireflies and Fireworks

FFI Start	FFI End	Cameras	Description
2020021225922	2020021232922	2	Fireflies
2020022112922	2020022115922	2, 3	Firefly
2020027032922	2020027035922	1, 2, 3	Fireworks
2020031012922	2020031015922	2	Firefly
2020033052922	2020033065922	1, 2, 3, 4	Fireworks
2020033115922	2020033122922	1	Firefly
2020038135922	2020038142922	2, 3, 4	Fireworks

transit depths are considerably larger.

A search for additional TCEs in potential multiple planet systems was conducted in DV through calls to TPS. A total of 936 TCEs were ultimately identified in the SPOC pipeline on 638 unique target stars. Table 3 provides a breakdown of the number of TCEs by target. Note that targets with large numbers of TCEs are likely to include false positives.

Table 3: Sector 21 TCE Numbers

Number of TCEs	Number of Targets	Total TCEs
1	410	410
2	175	350
3	39	117
4	11	44
5	3	15
—	638	936

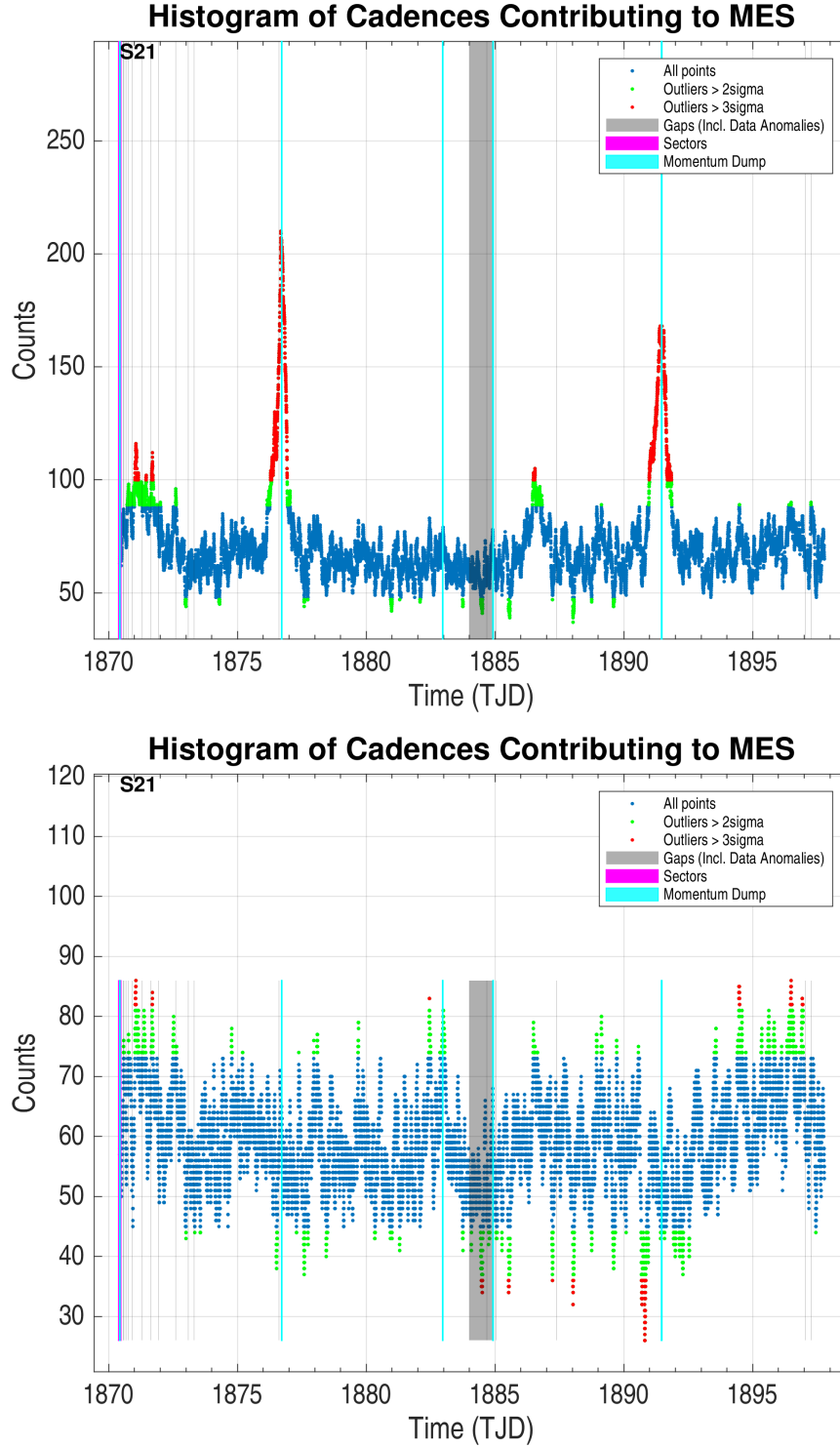


Figure 7: Top panel: Number of TCEs at a given cadence exhibiting a transit signal, based on an initial run of TPS. Any isolated peaks are caused by single events that result in spurious TCEs. These peaks were used to define deemphasis weights that suppress problematic epochs for the transit detection statistics in a second iteration of TPS. Bottom panel: Results from the second run of TPS.

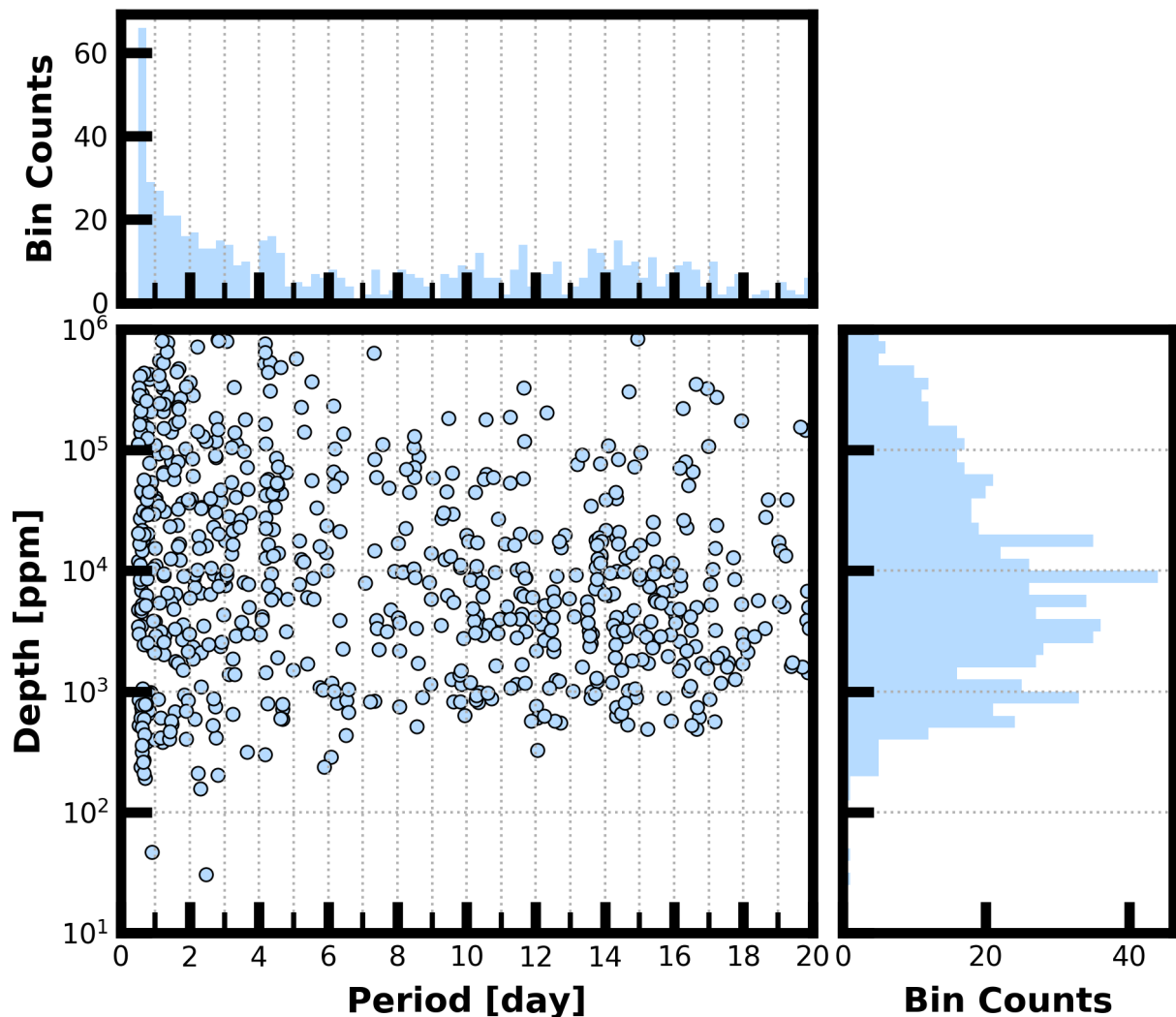


Figure 8: Lower Left Panel: Transit depth as a function of orbital period for the 936 TCEs identified for the Sector 21 search. For enhanced visibility of long period detections, TCEs with orbital period < 0.5 days are not shown. Reported depth comes from the DV limb darkened transit fit depth when available, and the DV trapezoid model fit depth when not available. Top Panel: Orbital period distribution of the TCEs shown in the lower left panel. Right Panel: Transit depth distribution for the TCEs shown in the lower left panel.

References

- Jenkins, J. M. 2017, [Kepler Data Processing Handbook](#): Overview of the Science Operations Center, Tech. rep., NASA Ames Research Center
- Jenkins, J. M., Twicken, J. D., McCauliff, S., et al. 2016, in Proc. SPIE, Vol. 9913, Software and Cyberinfrastructure for Astronomy IV, [99133E](#), doi: [10.1117/12.2233418](#)
- Li, J., Tenenbaum, P., Twicken, J. D., et al. 2019, *PASP*, 131, 024506, doi: [10.1088/1538-3873/aaf44d](#)
- Twicken, J. D., Catanzarite, J. H., Clarke, B. D., et al. 2018, *PASP*, 130, 064502, doi: [10.1088/1538-3873/aab694](#)
- Vanderspek, R., Doty, J., Fausnaugh, M., et al. 2018, [TESS Instrument Handbook](#), Tech. rep., Kavli Institute for Astrophysics and Space Science, Massachusetts Institute of Technology

Acronyms and Abbreviation List

BTJD Barycentric-corrected TESS Julian Date

CAL Calibration Pipeline Module

CBV Cotrending Basis Vector

CCD Charge Coupled Device

CDPP Combined Differential Photometric Precision

COA Compute Optimal Aperture Pipeline Module

CSCI Computer Software Configuration Item

CTE Charge Transfer Efficiency

Dec Declination

DR Data Release

DV Data Validation Pipeline Module

DVA Differential Velocity Aberration

FFI Full Frame Image

FIN FFI Index Number

FITS Flexible Image Transport System

FOV Field of View

FPG Focal Plane Geometry model

KDPH Kepler Data Processing Handbook

KIH Kepler Instrument Handbook

KOI Kepler Object of Interest

MAD Median Absolute Deviation

MAP Maximum A Posteriori

MAST Mikulski Archive for Space Telescopes

MES Multiple Event Statistic

NAS NASA Advanced Supercomputing Division

PA Photometric Analysis Pipeline Module

PDC Pre-Search Data Conditioning Pipeline Module

PDC-MAP Pre-Search Data Conditioning Maximum A Posteriori algorithm

PDC-msMAP Pre-Search Data Conditioning Multiscale Maximum A Posteriori algorithm

PDF Portable Document Format

POC Payload Operations Center

POU Propagation of Uncertainties

ppm Parts-per-million

PRF Pixel Response Function

RA Right Ascension

RMS Root Mean Square

SAP Simple Aperture Photometry

SDPDD Science Data Products Description Document

SNR Signal-to-Noise Ratio

SPOC Science Processing Operations Center

SVD Singular Value Decomposition

TCE Threshold Crossing Event

TESS Transiting Exoplanet Survey Satellite

TIC TESS Input Catalog

TIH TESS Instrument Handbook

TJD TESS Julian Date

TOI TESS Object of Interest

TPS Transiting Planet Search Pipeline Module

UTC Coordinated Universal Time

WCS World Coordinate System

XML Extensible Markup Language